HTML ABSTRACT + LINKS

Stark absorption spectroscopy of indole and 3-methylindole

Erko Jalviste[a)]
Institute of Physics, University of Tartu, Riia 142, 51014 Tartu, Estonia

Nobuhiro Ohta[b)]
Research Institute for Electronic Science (RIES), Hokkaido University, Sapporo 060-0812, Japan

(Received 7 May 2004; accepted 18 June 2004)

Indole and 3-methylindole (3-MI) doped into a polymethylmethacrylate (PMMA) film are studied by the Stark absorption (electroabsorption) spectroscopy. The ^1L_a and ^1L_b absorption bands are distinguished and the change in permanent dipole moment on ^1L_a excitation is determined by a model fit to the measured absorption and electroabsorption spectra. Analysis of the spectra, measured at normal incidence and magic angle conditions, proved the essential role of the electric-field-induced orientation/alignment effects for polar indole and 3-MI molecules in the PMMA environment at room temperature. © *2004 American Institute of Physics.*
[DOI: 10.1063/1.1782076]

I. INTRODUCTION

The importance of the research on the electronic structure and dynamics of indole and its derivatives stems from the fact that indole is a chromophore of the amino acid tryptophan. Tryptophan fluorescence is widely used for characterizing the structure and dynamics of the surrounding protein environment.[1–3] 3-methylindole (3-MI) is of particular interest, since the methyl group has nearly the same effect on indole ring as the alanyl group, and the absorption spectrum of 3-MI in solution is very similar to that of tryptophan.[4,5]

The absorption spectrum of indoles in near ultraviolet region is formed by two overlapping transitions from the ground state to the $\pi\pi^*$-type excited electronic states ^1L_a and ^1L_b. The blue end of the ^1L_a band is, in turn, partially overlapped with the rising edge of the strong $\pi\pi^*$-type ^1B_b band. In the room-temperature solution spectra the ^1L_a band is stronger and less structured than the ^1L_b band. Numerous investigations on the solvatochromism of indoles (see, e.g., Refs. 6–9 and references therein) confirmed that the ^1L_a state is more sensitive to the solvent polarity than the ^1L_b state. This fact is explained by a much larger permanent dipole moment in the ^1L_a state than that in the ^1L_b state.[6,10]

Apart from the solvatochromism, a more straightforward method for determining the change in dipole moment $\Delta\mu$ and the change in average polarizability $\Delta\alpha$ on an electronic excitation is the Stark absorption (electroabsorption, EA) spectroscopy,[11–14] where a small absorption change induced by an externally applied electric field is measured. For an ensemble of mobile polar molecules also the parameters characterizing the field-induced orientation and alignment can be obtained. The desired molecular parameters are obtained by fitting the absorption and EA spectra to a Stark effect model, which is usually a selected subset of the Liptay's equations,[11–14] describing the external-field-induced absorption change in solutions.

Pierce and Boxer[15] studied several tryptophan derivatives (*N*-acetyl-*L*-tryptophanamide (NATA), melittin, and 5-methoxytryptophan) dissolved into polar solvents at liquid nitrogen temperature by EA spectroscopy. For the decomposition of the absorption and EA spectra to the ^1L_a and ^1L_b components, the fluorescence polarization anisotropy excitation (FPAE) spectrum was recorded. The absorption, EA, and FPAE spectra were then simultaneously fit to the Stark effect model incorporating the decomposition procedure of Valeur and Weber.[16–18] The shapes of the ^1L_a and ^1L_b bands, the corresponding dipole changes $\Delta\mu_{L_a}$ and $\Delta\mu_{L_b}$, and several other molecular parameters were determined from the fit. The obtained $\Delta\mu_{L_a}$ and $\Delta\mu_{L_b}$ values (without the internal field correction) were 5.9 and 1.5 D for NATA and 6.2 and 1.1 D for melittin, respectively. However, the measured data were limited to the wavelength greater than 286 nm.

In the present study, room-temperature absorption and EA spectra of indole and 3-MI, doped into a spin-coated polymethylmethacrylate (PMMA) film, were measured and analyzed using a model fit. We were able to cover the wavelength range down to 230 nm. Recognizing that indole and 3-MI are not completely immobilized in a room-temperature PMMA film, we examined carefully the effect of sample angle on the EA spectra in order to comprehend the field-induced orientation/alignment effects. Unlike Pierce and Boxer[15] we did not use FPAE spectroscopy. Nevertheless, through a proper selection of the assumptions implemented in our Stark effect model we succeeded in reproducing the measured spectra, distinguishing between the ^1L_a and ^1L_b bands, and gaining information on the magnitude and the direction of $\boldsymbol{\Delta\mu}_{L_a}$ vector for indole and 3-MI.

II. EXPERIMENT

For EA measurements with polarized light, the experimental setup used in our previous EA studies[19–21] was complemented with a prism polarizer and a rotatable sample holder.

[a)]Electronic mail: erko@fi.tartu.ee
[b)]Electronic mail: nohta@es.hokudai.ac.jp

 © 2004 American Institute of Physics

Downloaded 25 Aug 2004 to 129.100.61.167. Redistribution subject to AIP license or copyright, see http://jcp.aip.org/jcp/copyright.jsp

A PMMA film containing indole or 3-MI was prepared by spin coating on a silica glass slide partially precoated with a conductive indium-tin-oxide (ITO) layer. The ratio of the number of moles of indole (or 3-MI) to the number of moles of PMMA monomer units (the molar ratio) was chosen to be 0.15 in order to obtain the absorbance of about 0.4 optical density (O.D.) units at the band center. After spin coating the sample slides were dried at room temperature about 24 h and stored in a refrigerator in order to minimize the evaporation of indole (or 3-MI) out of the PMMA layer. Indole (Tokyo Kasei Chemicals), 3-MI (Tokyo Kasei Chemicals), spectroscopic grade benzene (Waco Chemicals) and PMMA (Aldrich, molecular weight = 120 000) were used without further purification.

The thickness of the PMMA layer (typically about 0.5 μm) was measured with an interferometric microscope (NanoSpec/AFT 010-0180 from Nanometrics). A semitransparent aluminum film was vacuum deposited on the indole-doped (or 3-MI-doped) PMMA layer. ITO and aluminum layers were used as the Stark electrodes to which the wires were attached with a silver paste. The applied 40 Hz ac Stark voltage was set proportionally to the thickness of the sample film. This ensured the same field strength of 1 MV/cm rms for different samples.

Absorption spectra were measured with Hitachi U-3500 spectrometer using the resolution of 1.5 nm. For EA measurements the converging light beam from JASCO FP777 fluorescence spectrometer was collimated with a pinhole ($d = 1.4$ mm) and a lens ($f = 20$ mm) and directed through a 10 mm aperture α-BBO polarizing prism (JDSU CASIX) and through the sample slide on an external photomultiplier. A rotary stage was used for varying the angle between the sample slide and the light beam. The resolution of the spectrometer was set to 1.5 nm. The absorption measurements as well as the EA measurements were performed at room temperature.

The signal from the photomultiplier was amplified and divided into two channels. The dc component reflecting the transmitted light intensity was recorded directly by a personal computer. The ac component was directed to a lock-in amplifier (SR830, SRS) detecting the signal at the *second harmonic* of Stark field alternation frequency ω. In this way the response scaling quadratically with the field strength is extracted. The amplitude and the phase signals from the output of the lock-in amplifier, which give the external field induced transmission change $\Delta I(\lambda,2\omega)$, were digitized and recorded by a personal computer together with the dc component. To avoid the signal underflow or overflow in EA measurements the spectra were recorded in two parts, where the longer wavelength part was measured with a neutral attenuation filter, inserted into the path of the light beam.

The measured ΔI and I values are related to the absorbance change $\Delta A = A(\lambda,F) - A(\lambda,F=0)$ by[11,14]

$$\Delta A = -(2\sqrt{2}/\ln 10)\Delta I(\lambda,2\omega)/I(\lambda), \tag{1}$$

where the factor $2\sqrt{2}$ converts the value of measured rms $\Delta I(2\omega)$ signal to its value as if measured with static Stark field and the factor $1/\ln 10$ comes from the definition of the absorbance, $A = -\log I/I_0$.

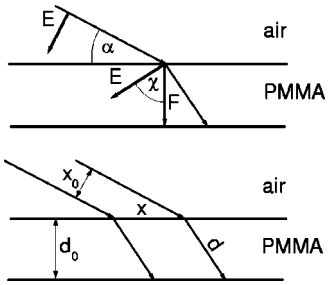

FIG. 1. Upper panel illustrates Snell's law relation between the angles α and χ, $\cos\alpha = n\cos\chi$, where α is the angle between the light beam and the sample slide and χ is the angle between the electric field vectors **E** (of the light) and **F** (of the applied field) in the PMMA layer. Lower panel explains the physical meaning of the quantities $1/\sin\chi = d/d_0$ and $1/\sin\alpha = x/x_0$, which describe the lengthening of the optical path in the PMMA layer and the lengthening of the light spot on the sample, respectively.

The wavelength scale of the EA spectrometer was calibrated relative to the scale of the absorption spectrometer with the help of naphthalene spectra. The EA spectrum of naphthalene had five nodes in the spectral region from 250 to 300 nm, which served as reference points. The first-derivative curve calculated from the absorption spectrum was found to be 1.9 nm blueshifted from the measured EA spectrum. This 1.9 nm shift was used as an apparatus constant in the analysis of the spectra of indole and 3-MI.

The EA spectra as well as the absorption spectra of indole and 3-MI were measured at four different angles α between the sample slide and the beam of the probe light, see Fig. 1 and Table I. The selected α values correspond to the $3\cos^2\chi - 1$ factor of 0.2, 0, -0.5, and -1, where χ is the angle between the applied electric field **F** and the electric field of light **E** in the PMMA layer. For light polarized in the incidence plane, the angles α and χ must obey Snell's law

$$\cos\alpha = n\cos\chi, \tag{2}$$

where n is the refraction index of PMMA. Its value, read out form the plot in Ref. 22, is 1.544 at 270 nm and 1.536 at 300 nm. The data in Table I were calculated using $n = 1.544$.

III. THEORY AND MODELING

A. Theory of Stark absorption spectroscopy

The change in transition frequency of a molecule subjected to an electric field **F** is given by

$$h\Delta\nu = -\Delta\boldsymbol{\mu}\cdot\mathbf{F} - (1/2)\mathbf{F}\cdot\Delta\boldsymbol{\alpha}\cdot\mathbf{F}, \tag{3}$$

TABLE I. Values of some parameters of the Stark effect model at four different sample angles used in the measurements. The physical meaning of χ, α, $1/\sin\chi$, and $1/\sin\alpha$ is illustrated in Fig. 1. $3\cos^2\chi - 1 = 0$ condition defines the magic value of the χ angle. The refraction index of PMMA is assumed to be 1.544 at $\lambda = 270$ nm (Ref. 22).

$3\cos^2\chi - 1$	χ	α	$1/\sin\chi$	$1/\sin\alpha$
0.2	50.7°	12°	1.29	4.64
0	54.7°	27°	1.22	2.20
−0.5	65.9°	51°	1.09	1.29
−1	90°	90°	1	1

Downloaded 25 Aug 2004 to 129.100.61.167. Redistribution subject to AIP license or copyright, see http://jcp.aip.org/jcp/copyright.jsp

where $\Delta\boldsymbol{\mu}$ and $\Delta\boldsymbol{\alpha}$ are the change in permanent dipole moment vector and the change in polarizablity tensor on the transition, respectively.

In case of overlapping absorption bands the absorbance and the field-induced change in absorbance are the sum of the contributions from participating electronic transitions:

$$A=\sum_i A_i, \quad \Delta A=\sum_i \Delta A_i. \tag{4}$$

According to the Stark effect theory of Liptay[11–14] the field-induced change in absorbance for the ith transition ΔA_i, averaged over the angular distribution of molecules, can be expressed as a sum of zeroth, first, and second derivatives by the frequency from A_i/ν,

$$\Delta A_i=(fF)^2\left[a_iA_i+b_i\nu\frac{d(A_i/\nu)}{d\nu}+c_i\nu\frac{d^2(A_i/\nu)}{d\nu^2}\right], \tag{5}$$

where f is the internal field factor, and F is the strength of the applied electric field. Neglecting the transition moment polarizabilities and assuming the excited and ground state polarizabilities isotropic the coefficients a_i, b_i, and c_i can be expressed as[11–14]

$$a_i=(\mu^2/30k^2T^2)(3\cos^2\chi-1)[3\cos^2(\boldsymbol{\mu}\angle\mathbf{d}_i)-1], \tag{6}$$

$$b_i=\Delta\alpha_i/2h+(\mu\Delta\mu_i/3hkT)\cos(\Delta\boldsymbol{\mu}_i\angle\boldsymbol{\mu}) +(\mu\Delta\mu_i/15hkT)(3\cos^2\chi-1) \times[3\cos(\Delta\boldsymbol{\mu}_i\angle\mathbf{d}_i)\cos(\boldsymbol{\mu}\angle\mathbf{d}_i)-\cos(\Delta\boldsymbol{\mu}_i\angle\boldsymbol{\mu})], \tag{7}$$

$$c_i=\Delta\mu_i^2/6h^2+(\Delta\mu_i^2/30h^2)(3\cos^2\chi-1) \times[3\cos^2(\Delta\boldsymbol{\mu}_i\angle\mathbf{d}_i)-1], \tag{8}$$

where μ is the dipole moment in the ground electronic state, $\Delta\mu_i$ is the change in the dipole moment and $\Delta\alpha_i$ is the change in average polarizability on the transition from the ground state to the ith excited electronic state, $\mathbf{d}_i$ is the transition dipole moment of ith transition, χ is the angle between the electric field vectors of the absorbing light $\mathbf{E}$ and of the applied electric field $\mathbf{F}$, and T is the temperature of the sample. The other angles are designated by the symbol $\angle$, for instance, $\Delta\boldsymbol{\mu}_i\angle\boldsymbol{\mu}$ is the angle between the dipole change and the ground state dipole.

Equations (1), (4)–(8) provide a link between the measured quantities $[A(\lambda),F,\chi,I(\lambda),\Delta I(\lambda),T]$ and the parameters characterizing the molecule $(\Delta\mu_i,\Delta\alpha_i,\mu,\boldsymbol{\mu}\angle\mathbf{d}_i,\Delta\boldsymbol{\mu}\angle\mathbf{d}_i,\ldots)$.

The zeroth-derivative contribution to the absorption change [Eqs. (5) and (6)] arises from the deviation of the distribution of the ensemble of transition dipoles from isotropy owing to the alignment of the ground state dipoles along the field direction. The first-derivative contribution [Eqs. (5) and (7)] arises from the Stark shift of the absorption band owing to the polarizability change [Eq. (3)], and by the concerted effect of the field-induced orientation of ground state dipoles and the Stark shift caused by the dipole change [Eq. (3)]. For an orientated ensemble, where the number of molecules with redshifted absorption band is larger than the number of molecules with blueshifted band, the ensemble average results in an effective redshift. The second-derivative contribution [Eqs. (5) and (8)] arises from the effective field-induced broadening of the absorption band owing to the Stark shift caused by dipole change [Eq. (3)]. The broadening results from the average over an ensemble containing equal number of molecules with blueshifted and redshifted absorption band.

It should be kept in mind that the Stark effect theory[12] is based on several simplifying assumptions:

(1) For individual molecules subjected to the electric field, the absorption band of a given electronic transition can shift in the frequency scale, but does not alter its shape. The apparent change of the band shape is the result of ensemble average over the molecules experiencing different Stark shifts.

(2) The absorption features are much broader than the Stark shift.

(3) The angular distribution of molecules without the external field is isotropic.

(4) The applied field is not too strong to induce orientational saturation, i.e., $\mu F/kT\ll 1$.

(5) The angular motion of the molecules is fast enough to follow a time-varying Stark field, i.e., the angular distribution for an instantaneous field strength is the same as for a static field with the same strength. The opposite limit case of an immobile isotropically distributed ensemble of embedded molecules can be modeled by neglecting the orientation/alignment terms including the $1/kT$ factor.

B. Stark effect model for indole and 3-MI

In Eqs. (6), (7), and (8) the polarizabilty anisotropy and the transition moment polarizability contributions are already neglected, because it is difficult to distinguish these minor effects from the dominating dipole-induced effects. The transition moment polarizability effects become evident for bigger and highly polar ($\mu>10$ D) donor/acceptor-substituted ''push-pull'' molecules, which show a significant charge transfer on excitation.[23,24] Nevertheless, the Stark effect model given by Eqs. (4)–(8) is still too complicated to analyze the measured absorption and EA spectra of indole and 3-MI. Therefore, additional assumptions, simplifying the model and limiting the number of free parameters, were needed in order to achieve the convergence of the fit and to obtain physically meaningful results.

Stark effect measurements of gas-phase indole[25] resulted $\Delta\mu_{L_b}$ to be only of 0.14 D. Complete active space (CASSCF) *ab initio* calculations for indole at its ground state geometry[26] yielded the following values of dipole moments: $\mu=1.87$ D, $\mu_{L_b}=1.55$ D, and $\mu_{L_a}=6.12$ D. These results suggest that $\Delta\mu_{L_b}$ can be more than an order of magnitude smaller than $\Delta\mu_{L_a}$. Therefore, we assumed that $\Delta\mu_{L_b}=0$ in Eqs. (7) and (8). We also assumed that $\Delta\mu_{B_b}=0$, because it is sufficient to use a single parameter $(\Delta\alpha_{B_b})$ to describe the low-frequency ending of the ^1B_b band.

For the ^1L_a band, which dominates in the absorption and EA spectra, the dipole contributions cannot be neglected. Further simplification of the model is still possible by the

Downloaded 25 Aug 2004 to 129.100.61.167. Redistribution subject to AIP license or copyright, see http://jcp.aip.org/jcp/copyright.jsp

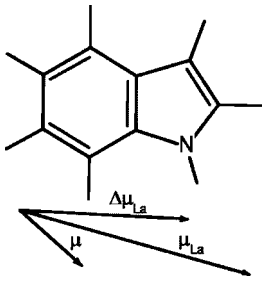

FIG. 2. Directions of the ^1L_a state dipole moment $\boldsymbol{\mu}_{L_a}$, the ground state dipole moment $\boldsymbol{\mu}$, and their difference $\boldsymbol{\Delta\mu}_{L_a}$ for indole. The $^1L_a \leftarrow S_0$ transition dipole moment is assumed to be parallel with $\boldsymbol{\mu}$, but the $^1L_b \leftarrow S_0$ transition dipole moment is assumed to be perpendicular with $\boldsymbol{\mu}$.

predetermination of some molecular angles based on available literature data.

The projections of the ground state dipole moment of indole to its principal inertial axes ($\mu_a = 1.59$ D and $\mu_b = 1.36$ D) determined by gas-phase microwave spectroscopy[27] correspond to the angle of 40.5° between $\boldsymbol{\mu}$ and the long molecular axis of indole. The direction of $\boldsymbol{\mu}$, shown in Fig. 2, is chosen guided by the results of *ab initio* calculations,[26,28] which predicted that $\boldsymbol{\mu}$ points towards the nitrogen atom and makes an angle of 47° with the long axis. Linear dichroism measurements of indole doped into a stretched polymer film[29] resulted 46° and *ab initio* calculations[30,31] resulted 36° for the angle between the long axis and the $^1L_a \leftarrow S_0$ transition dipole moment $\mathbf{d}_{L_a}$. On the basis of these data we assumed in our model that $\mathbf{d}_{L_a}$ is parallel to $\boldsymbol{\mu}$, i.e., $\boldsymbol{\mu} \angle \mathbf{d}_{L_a} = 0°$.

For indole the angle between the $^1L_b \leftarrow S_0$ transition moment $\mathbf{d}_{L_b}$ and the long axis (towards the carbon atom in the third position) is determined to be 38.3° from the rotationally resolved spectrum of the ^1L_b band origin[32] and 42° from the linear dichroism measurements,[29] in agreement with the *ab initio* predictions.[30,31] Therefore we assumed for simplicity that $\mathbf{d}_{L_b}$ makes a right angle with $\boldsymbol{\mu}$.

Since the dipolar orientation/alignment effects turned out to be essential to interpret the EA spectra of indole and 3-MI, the a_{L_a} and a_{L_b} coefficients [Eq. (6)] are retained in our model. The $^1B_b \leftarrow S_0$ transition dipole of indole is tilted from the long axis by 7° towards the carbon atom[29] and makes thus nearly magic angle with the ground state dipole moment. This justifies the neglect of the a_{B_b} coefficient.

In the Stark effect model accommodated to indole the nonzero coefficients for the transitions to the ^1L_a, ^1L_b, and ^1B_b states entering into Eq. (5) are then given by

$$a_{L_a} = (\mu^2/15k^2T^2)(3\cos^2\chi - 1), \tag{9}$$

$$b_{L_a} = \Delta\alpha_{L_a}/2h + (\mu\Delta\mu_{L_a}/3hkT) r \cos\gamma + (2\mu\Delta\mu_{L_a}/15hkT) r\cos\gamma(3\cos^2\chi - 1), \tag{10}$$

$$c_{L_a} = \Delta\mu_{L_a}^2/6h^2 + (\Delta\mu_{L_a}^2/30h^2)(3\cos^2\gamma - 1) \times (3\cos^2\chi - 1), \tag{11}$$

$$a_{L_b} = (-\mu^2/30k^2T^2)(3\cos^2\chi - 1), \tag{12}$$

$$b_{L_b} = \Delta\alpha_{L_b}/2h, \tag{13}$$

$$b_{B_b} = \Delta\alpha_{B_b}/2h, \tag{14}$$

where $\gamma = \boldsymbol{\Delta\mu}_{L_a} \angle \boldsymbol{\mu} = \boldsymbol{\Delta\mu}_{L_a} \angle \mathbf{d}_{L_a}$ and r is an extra dimensionless parameter weighting the dipole terms of the b_{L_a} coefficient. Its physical meaning is explained in Sec. V A.

Thus, seven parameters are needed to be determined by the model fit: μ, $\Delta\alpha_{L_a}$, $\Delta\mu_{L_a}$, $\cos\gamma$, $\Delta\alpha_{L_b}$, $\Delta\alpha_{B_b}$, and r. The a_{L_a}, b_{L_a}, and c_{L_a} coefficients can be expressed as a sum of a constant term and a term being proportional to $3\cos^2\chi - 1$,

$$a_{L_a} = a_2(3\cos^2\chi - 1), \tag{15}$$

$$b_{L_a} = b_1 + b_2(3\cos^2\chi - 1), \tag{16}$$

$$c_{L_a} = c_1 + c_2(3\cos^2\chi - 1). \tag{17}$$

A comparison of Eqs. (15), (16), and (17) with Eqs. (9), (10), and (11) indicates that there are no redundant or missing parameters in the proposed parameter set. For example, μ is determined by a_2, $\Delta\mu_{L_a}$ and $\cos\gamma$ are determined by c_1 and c_2. Subsequently, r and $\Delta\alpha_{L_a}$ are determined by b_1 and b_2 if μ_{L_a}, $\Delta\mu_{L_a}$, and $\cos\gamma$ are known. This also implies that the possible contributions of other physical origin to the EA spectrum, for instance, the polarizability anisotropy or the transition moment polarizability are "absorbed" into the given model parameters.

The ground state dipole moment of 3-MI calculated at B3LYP 6-31+G* level is of 2.06 D.[33] Solvatochromic data[6] suggest that the values of excited state permanent dipoles of 3-MI are close to those of indole. Linear dichroism measurements[29] showed that the transition dipole moment angles of 3-MI with respect to the indole chromophore differed only few degrees from the corresponding angles of indole. Relying on the similarity of the electronic properties of indole and 3-MI we applied the Stark effect model of indole also to 3-MI.

C. Data processing

Although the ^1L_a and ^1L_b band shapes for indole are available from the literature,[16–18] they cannot be directly used because the deconvoluted spectrum is measured at different conditions. For instance, the spectrum of indole in propylene glycol at −60 °C obtained by Rich *et al.*[18] is more structured than the room-temperature spectrum of indole in PMMA. The differences in the shape will be even more pronounced for the first and second derivative curves, which are required for the simulation of the electroabsorption spectra. Therefore, in this work, following the method of Pierce and Boxer,[15] both the parameters of the Stark effect model and the parameters describing the shape of the ^1L_a, ^1L_b, and ^1B_b bands are determined by a least-square fit to the observed absorption and EA spectra.

The shape of each absorption band A_i is described as a sum of Gaussian functions as

Downloaded 25 Aug 2004 to 129.100.61.167. Redistribution subject to AIP license or copyright, see http://jcp.aip.org/jcp/copyright.jsp

$$A_i(\lambda)=\sum_j G_{ij}(\lambda)=\sum_j \sqrt{\frac{2}{\pi}}\frac{a_{ij}}{w_{ij}}\exp\left(-\frac{2(\lambda-\lambda_{ij}^0)^2}{w_{ij}^2}\right), \tag{18}$$

where the index i labels the ${}^1L_a$, ${}^1L_b$, or ${}^1B_b$ band, and the index j distinguishes individual Gaussians of a given band. Each Gaussian is defined by its center wavelength λ^0, its width w, and its area a. As the measured absorption and EA data are given in the wavelength scale we avoided forth- and back-conversions, to the frequency scale in the analysis. Thus, the first and second derivatives for the ith band entering into Eq. (5) are calculated as $\Sigma_j \nu d[G_{ij}(\lambda)/\nu]/d\nu$ and $\Sigma_j \nu d^2[G_{ij}(\lambda)/\nu]/d\nu^2$, respectively, where

$$\nu\frac{d[G_{ij}(\lambda)/\nu]}{d\nu}=-\lambda^2\frac{dG_{ij}(\lambda)}{d\lambda}-\lambda G_{ij}(\lambda), \tag{19}$$

$$\nu\frac{d^2[G_{ij}(\lambda)/\nu]}{d\nu^2}=\lambda^4\frac{d^2G_{ij}(\lambda)}{d\lambda^2}+4\lambda^3\frac{dG_{ij}(\lambda)}{d\lambda}+2\lambda^2G_{ij}(\lambda). \tag{20}$$

The analytical expressions of $dG_{ij}(\lambda)/d\lambda$ and $d^2G_{ij}(\lambda)/d\lambda^2$ can be obtained by direct differentiation.

Optimal choice was the $1+3+2$ basis set of Gaussians, where a single Gaussian models the rising edge of the ${}^1B_b$ band, three Gaussians model the ${}^1L_a$ band, and two Gaussians model the ${}^1L_b$ band. Smaller number of Gaussians led to insufficient description of spectra, but larger number rendered the fit unstable. Initial values of the areas, width, and center frequencies of the Gaussians were adjusted in a way that the simulated ${}^1L_a$ and ${}^1L_b$ band shapes resembled the band shapes determined from the fluorescence anisotropy measurements.[16–18] For instance, the first kink in the red part of the absorption spectra recognized as the ${}^1L_b$ band origin was associated to a ${}^1L_b$ Gaussian.

Simultaneous fit to the eight measured spectra of the same sample was performed. The eight spectra included four absorption spectra and four EA spectra measured with the angle α of 90°, 51°, 27°, and 12° (Table I). Altogether, the spectra of indole and 3-MI contained 1288 and 1368 data points, respectively. The simulated absorption and EA spectra for α smaller than 90° were weighted by the corresponding optical path factor $1/\sin\chi$ (Table I). The proportionality between the absorbance change ΔA and the path factor $1/\sin\chi$ can be rationalized as follows: the transmitted intensity I decreases proportionally to the optical path length, but the field-induced change of the transmitted intensity ΔI remains constant, since its increase is compensated by the decreased transmission.

Numerous trial fits and visual checks of the simulated spectra were carried out to find a set of parameters and their initial values, which does not lead to a physically inconsistent result. In the final fit altogether 24 variable parameters were used, including μ, $\Delta\mu_{L_a}$, $\cos\gamma$, r, $\Delta\alpha_{L_a}$, $\Delta\alpha_{L_b}$, $\Delta\alpha_{B_b}$, the areas, widths, and the center wavelengths of the six $(1+3+2)$ Gaussian functions (except for the center wavelength of the ${}^1B_b$ Gaussian, which was fixed).

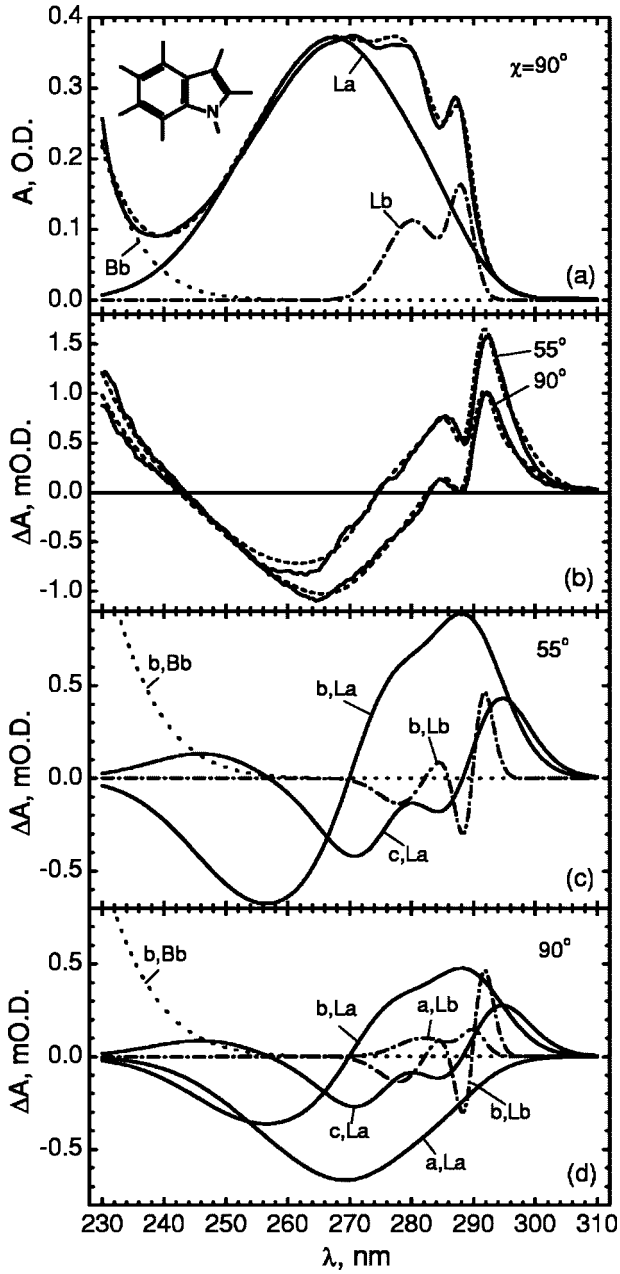

FIG. 3. (a) Observed absorption spectrum (solid curve), simulated absorption spectrum (dashed curve), and its decomposition to the ${}^1L_a$, ${}^1L_b$, and ${}^1B_b$ bands (labeled curves) for indole in PMMA; (b) observed (solid curves) and simulated (dashed curves) electroabsorption (EA) spectra for indole in the magic angle case ($\chi=55°$) and in the normal incidence case ($\chi=90°$); (c) the b_{L_a}, c_{L_a}, b_{L_b}, and b_{B_b} components of the simulated EA spectrum in the magic angle case; (d) the a_{L_a}, b_{L_a}, c_{L_a}, a_{L_b}, b_{L_b}, and b_{B_b} components of the simulated EA spectrum in the normal incidence case. The letters a, b, and c designate the zeroth-, the first-, and the second-derivative contributions, respectively. The absorbance and its change are given in dimensionless optical density units.

The uncertainty of the EA data points was set to 0.1 mO.D. (10^{-4} optical density units) and the uncertainty of the absorbance data points was set to 15 mO.D.. Smaller uncertainty for the absorbance data points relative to the uncertainty of the EA data points resulted in a better reproduction of the absorption spectra, but a poorer reproduction of the EA spectra and *vice versa*.

Downloaded 25 Aug 2004 to 129.100.61.167. Redistribution subject to AIP license or copyright, see http://jcp.aip.org/jcp/copyright.jsp

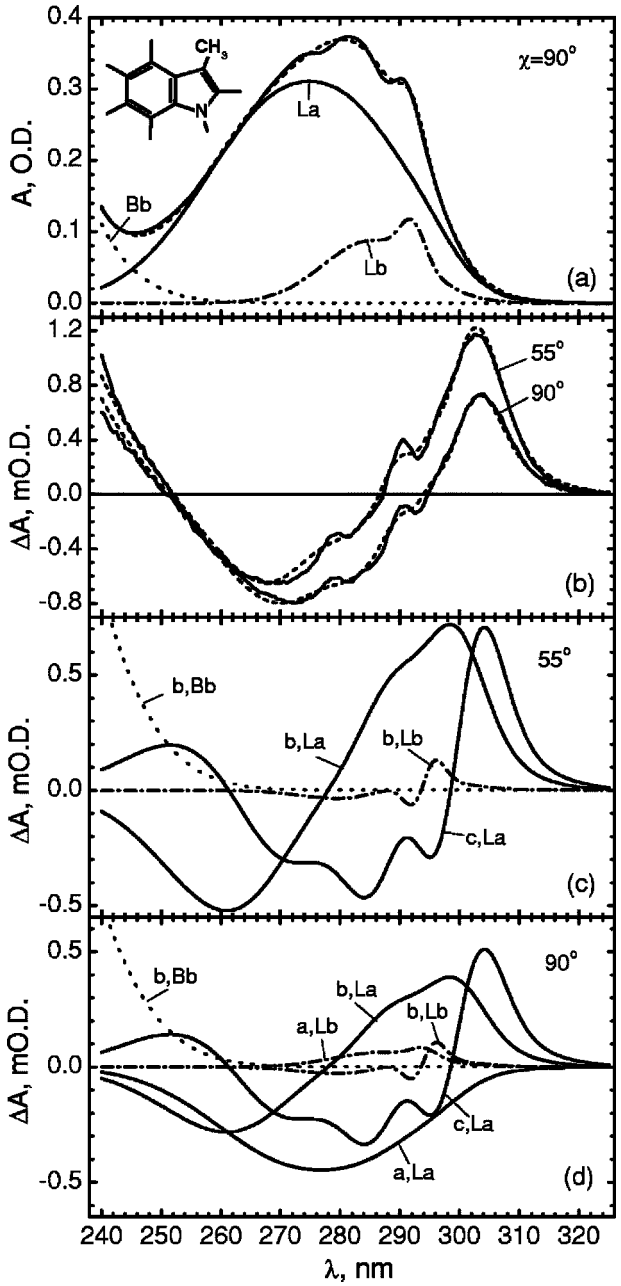

FIG. 4. (a) Observed absorption spectrum (solid curve), simulated absorption spectrum (dashed curve), and its decomposition to the ^1L_a, ^1L_b, and ^1B_b bands (labeled curves) for 3-methylindole in PMMA; (b) observed (solid curves) and simulated (dashed curves) electroabsorption (EA) spectra for 3-methylindole in the magic angle case ($\chi=55°$) and in the normal incidence case ($\chi=90°$); (c) the b_{L_a}, c_{L_a}, b_{L_b}, and b_{B_b} components of the simulated EA spectrum in the magic angle case; (d) the a_{L_a}, b_{L_a}, c_{L_a}, a_{L_b}, b_{L_b}, and b_{B_b} components of the simulated EA spectrum in the normal incidence case. The letters a, b, and c designate the zeroth-, the first-, and the second-derivative contributions, respectively. The absorbance and its change are given in dimensionless optical density units.

TABLE II. Molecular parameters from the model fit to the measured absorption and electroabsorption spectra of indole and 3-methylindole.[a,b,c]

	Indole	3-MI	
$\Delta\mu_{L_a}$	5.6(2)	7.2(4)	D
$\cos\gamma$[d]	0.83(7)	0.72(6)	
$\Delta\alpha_{L_a}$	13(6)	13(10)	Å^3
$\Delta\alpha_{L_b}$	19(2)	10(5)	Å^3
μ[e]	1.42(3)	1.28(4)	D
r[f]	0.72(8)	0.64(9)	
γ[d]	34(7)	43(5)	deg
f_{L_b}/f_{L_a}[g]	0.13	0.16	
$\Delta\alpha_{L_a}^{\text{eff}}$[h]	90	83	Å^3

[a]The reported μ, $\Delta\mu_{L_a}$, $\Delta\alpha_{L_a}$, and $\Delta\alpha_{L_b}$ values are *not corrected* by the internal field factor.
[b]Fitted parameters with their uncertainties are given in the first six rows and derived parameters in the last three rows.
[c]$\Delta\mu_{L_b}$ was fixed to zero in the fit.
[d]$\gamma=\mu\angle\Delta\mu_{L_a}$.
[e]μ is the apparent ground state dipole moment reflecting the restricted character of field-induced alignment in PMMA, see Sec. V A.
[f]r characterizes the relative significance of orientation and alignment, see Eq. (10) and Sec. V A.
[g]f_{L_b}/f_{L_a} is the oscillator strength ratio calculated with Eq. (21).
[h]$\Delta\alpha_{L_a}^{\text{eff}}$ is an apparent polarizability change including the dipolar orientation contribution, calculated with Eq. (22).

IV. RESULTS

A. The measured spectra

Measured and simulated absorption spectra of indole and 3-MI are shown in Figs. 3(a) and 4(a), respectively. Only the normal-incidence-case ($\alpha=\chi=90°$) spectra are displayed. The other spectra, for which the sample angle α was smaller than 90°, had the same shape and their scaling factors agreed with the predicted ones given in Table I within 10%.

EA spectra of indole and 3-MI were measured with a field strength of 1 MV/cm (rms). The EA spectra measured in the normal incidence ($\alpha=\chi=90°$) and in the magic angle ($\alpha=27°$ and $\chi=55°$) conditions are shown in Figs. 3(b) and 4(b). For both indole and 3-MI, the EA curve for $\chi=66°$ lies between the curves for $\chi=55°$ and $\chi=90°$, and the EA curve for $\chi=51°$ lies above the curve for $\chi=55°$.

Some important conclusions can be made immediately from the observed EA spectra shown in Figs. 3(b) and 4(b):

(1) Field-induced increase in absorbance in the low-frequency (red) part of the EA curve indicates that the absorption band is redshifted in the presence of an external electric field.

(2) For the normal-incidence EA spectra the decrease in absorbance in the region of the absorption maximum is clearly dominating over the small increase in absorbance in the low-frequency part. This indicates a significant overall field-induced decrease in absorbance, caused by a nonvanishing zeroth derivative (a_i) contribution for some transition. The first-derivative (b_i) and the second-derivative (c_i) contributions, integrated over spectral range covering the whole band, must cancel out.

(3) For the magic-angle EA spectra the decrease in absorbance and the increase in absorbance seem to be balanced. The last two observations imply the presence of field-induced orientation/alignment of embedded molecules.

In spite of rather high sample concentration [0.15 moles of indole (3-MI) per mole of PMMA units corresponding to the number density of indole and 3-MI about 0.9×10^{21} cm^{-3}] no spectral evidence of complex formation was observed. Test measurements of the samples with ten times lower indole (3-MI) concentration showed that their

Downloaded 25 Aug 2004 to 129.100.61.167. Redistribution subject to AIP license or copyright, see http://jcp.aip.org/jcp/copyright.jsp

absorption and EA spectra, although being much noisier, had the same shape.

B. The model fit

The molecular parameters of indole and 3-MI determined in the present analysis are listed in Table II. With these parameters the measured absorption spectra [Figs. 3(a) and 4(a)] and the EA spectra [Figs. 3(b) and 4(b)] are reproduced reasonably well by the simulations. All the parameters determined by the fit (Table II) are in acceptable range. In Figs. 3(a) and 4(a) are also shown the shapes of the ^1B_b, ^1L_a, and ^1L_b bands, from which the simulated absorption spectra are composed of. Two Gaussians, from which the shape of the ^1L_b band is formed, are clearly recognizable. The three Gaussians of the ^1L_a band cause its first- and second-derivative curves [Figs. 3(c) and 4(c)] to be significantly different from the derivative curves of a single Gaussian.

The ratio between the $^1L_b \leftarrow S_0$ and $^1L_a \leftarrow S_0$ oscillator strengths, f_{L_b}/f_{L_a}, given in Table II is calculated numerically as the ratio between the areas covered by the corresponding absorption curves,

$$\frac{f_{L_b}}{f_{L_a}} = \frac{\int A_{L_b}(\nu)d\nu}{\int A_{L_a}(\nu)d\nu} = \frac{\int [A_{L_b}(\lambda)/\lambda^2]d\lambda}{\int [A_{L_a}(\lambda)/\lambda^2]d\lambda}. \tag{21}$$

The decomposition of the simulated EA spectra of indole and 3-MI to the ^1B_b, ^1L_a, and ^1L_b constituents, is shown in Figs. 3(c) and 4(c) in the magic angle case ($\chi = 55°$) and in Figs. 3(d) and 4(d) in the normal incidence case ($\chi = 90°$). There is no doubt about the presence of a large negative contribution proportional to the ^1L_a absorption in the latter case and its absence in the former case. This is a clear manifestation of the alignment of polar molecules indole and 3-MI along the electric vector of the applied field. Negative sign for the a_{L_a} component and positive sign for the a_{L_b} component in the $\chi = 90°$ case follow directly from the $3\cos^2(\boldsymbol{\mu} \angle \mathbf{d}_i) - 1$ factor in Eq. (6), being according to our model assumptions -2 for the $^1L_a \leftarrow S_0$ transition and 1 for the $^1L_b \leftarrow S_0$ transition.

Following Chowdhury *et al.*,[34] we evaluated also the apparent polarizability in the magic angle case $\Delta\alpha_{L_a}^{\text{eff}}$, including the electronic polarizability as well as the χ-independent dipolar orientational contribution. According to Eq. (10) it can be expressed as

$$\Delta\alpha_{L_a}^{\text{eff}} = \Delta\alpha_{L_a} + (2\mu\Delta\mu_{L_a}/3kT)r\cos\gamma, \tag{22}$$

where $\gamma = \mathbf{\Delta\mu}_{L_a} \angle \boldsymbol{\mu} = \mathbf{\Delta\mu}_{L_a} \angle \mathbf{d}_{L_a}$. The results are shown in Table II. Much larger value of $\Delta\alpha_{L_a}^{\text{eff}} - \Delta\alpha_{L_a}$ than that of $\Delta\alpha_{L_a}$ indicates that the dipolar orientational contribution dominates in the first-derivative b_{L_a} term.

Comparing Fig. 3(c) with Fig. 3(d) and Fig. 4(c) with Fig. 4(d), one can notice that the first-derivative b_{L_a} component is about twice larger in the magic angle case than in the normal incidence case. This is explainable by considering the χ dependence of the dipolar orientational contribution [Eq. (10)] and the optical path factor $1/\sin\chi$. Indeed, according to Eq. (16) the first-derivative contribution must be $(1/\sin\chi)b_1/(b_1 - b_2) = 2.0$ times larger in the magic angle case, where $3\cos^2\chi - 1 = 0$ and $1/\sin\chi = 1.22$ (Table I), than in the normal incidence case, where $3\cos^2\chi - 1 = -1$ and $1/\sin\chi = 1$. Here the factor $b_1/(b_1 - b_2)$ was estimated by using the approximate relation $b_2 = 0.4b_1$, which follows from Eq. (10) if the $\Delta\alpha_{L_a}$ contribution is neglected.

The uncertainties of the model parameters shown in Table II reflect the sensitivity of the fit quality to the variations of the parameters. Significant variations of loosely determined parameters changed the simulated spectra only a little bit. For example, satisfactory, but somewhat worse, agreement between the observed and simulated absorption and EA spectra of 3-MI was observed, even if both $\Delta\alpha_{L_b}$ and $\Delta\alpha_{L_a}$ were fixed to zero in the fit.

We also tested fitting with an extra Gaussian for the ^1L_b band, i.e., with the $1+3+3$ basis set. For indole this led to a better agreement between the simulated and the measured spectra. The shapes of the ^1L_a and ^1L_b bands were more similar to the shapes deduced from the fluorescence polarization anisotropy measurements[16–18] and the f_{L_b}/f_{L_a} oscillator strength ratio f_{L_b}/f_{L_a} was larger (0.34), being in a better agreement with the ratio deduced by a comparative analysis of the absorption spectra of different methyl-substituted indoles (0.36).[35] Nevertheless, we discarded these results because the fit resulted in an unacceptable $\Delta\alpha_{L_a}$ value of -50 Å^3. Actually, an overestimated dipolar orientational polarizability ($\Delta\mu_{L_a}$ was of 7.7 D) was compensated by negative electronic polarizability change. For 3-MI the inclusion of an extra Gaussian for the ^1L_b band did not improve the fit.

V. DISCUSSION

A. Field-induced orientation and alignment

The orientation/alignment effects for polar molecules doped into PMMA are investigated by EA spectroscopy in several works.[34,36,37] Their results are in excellent agreement with our observations.

Saal and Haase[36] measured the EA spectra of Disperse Red 1 azo dye ($\mu = 8.7$ D) embedded into a spin-coated PMMA film. The ground state and the transition dipole moments of the dye were assumed to be parallel. The applied electric field was directed along the light propagation. The angle χ was fixed to 90°, as can be inferred from their expression of the zero-derivative term. Measurements were performed at different sample temperatures and Stark field alternation frequencies ω. Analyzing the EA spectra, measured at a temperature of 105 °C, they observed the transition from mobile behavior for $\omega = 2$ Hz to immobile behavior for $\omega = 2$ kHz. Similarly to our data, the ''mobile'' EA spectrum was characterized by a significant negative zero-derivative contribution and about 3.3 times larger first-derivative contribution than those for the ''immobile'' spectrum.

Chowdhury *et al.*[34] studied magic angle EA spectra of Coumarin 153 ($\mu = 6.55$ D) in different host matrices. The Stark field alternation frequency of 450 Hz was used. They found that the EA spectrum of the room-temperature PMMA

Downloaded 25 Aug 2004 to 129.100.61.167. Redistribution subject to AIP license or copyright, see http://jcp.aip.org/jcp/copyright.jsp

samples depends strongly on the sample preparation method. For the samples heated 5 min at 150 °C the apparent measured polarizability change $\Delta\alpha^{\text{eff}}$ was about ten times smaller than for the samples dried for 24 h at room temperature. This was explained by a smaller rigidity of unheated PMMA, which leads to the dominance of the field-induced dipolar orientation effect over the electronic polarizability change. Moreover, for frozen organic solvent hosts the measured polarizability change was, in turn, an order of magnitude smaller, indicating that even for heated PMMA samples the embedded Coumarin 153 molecules are not completely immobilized at room temperature. Similar conclusions were in the EA study of all-trans retinal.[37] In order to avoid the evaporation of indole (3-MI) out of the PMMA layer we did not try to heat our samples.

Considering that the angular dependence of the energy of a dipole in an electric field is given by $-\mu F\cos(\boldsymbol{\mu}\angle\mathbf{F})$, the *equilibrium* angular distribution function for an ensemble of (ground state) dipoles in the electric field at a temperature T and its expansion to the Legendre polynomials (in case of $\beta\ll 1$) can be written as

$$W(\theta)=\exp(\beta\cos\theta)\approx 1+\beta P_1(\theta)+(1/3)\beta^2 P_2(\theta), \tag{23}$$

where $\theta=\boldsymbol{\mu}\angle\mathbf{F}$ and $\beta=\mu F/kT$. The Legendre polynomials $P_0(\theta)=1$, $P_1(\theta)=\cos\theta$, and $P_2(\theta)=(3/2)\cos^2\theta-1/2$ describe the isotropic, the *orientation*, and the *alignment* contribution to the angular distribution function, respectively. The alignment-type deviation from isotropy, proportional to F^2, gives rise to the zeroth-derivative term in the Stark effect theory [Eq. (6)] and the orientation-type deviation from isotropy, proportional to F, gives rise to the first-derivative term [Eq. (7)].

According to Eq. (23) low temperature should favor the orientation/alignment owing to the $\beta=\mu F/kT$ factor. This is indeed true in case of fast relaxation to the equilibrium angular distribution at a given field strength and temperature. In reality, the mobility of an indicator molecule and its local polymer surrounding, and therefore the field-induced orientation/alignment, is suppressed at lower temperatures. Intuitively, higher mobility, and consequently faster equilibration of the angular distribution, is expected for a less rigid host polymer, for lower Stark field alternation frequency, and for smaller size of embedded molecules. A host polymer is expected to be less rigid at higher temperature (especially above its glass transition temperature) and at higher concentration of the dopant molecules.

Following the idea of Saal and Haase[36] an unrelaxed time-varying angular distribution of dipoles can be regarded as an effective stationary distribution,

$$W(\theta)^{\text{unrel}}=1+q_1\beta P_1(\theta)+(1/3)q_2^2\beta^2 P_2(\theta), \tag{24}$$

where the empirical coefficients $q_1(\omega,T)$ and $q_2(\omega,T)$ depend on the Stark field alternation frequency ω and the sample temperature T. In the limit of a mobile ensemble of dipoles, whose distribution follows the field in a full extent, $q_1=q_2=1$. In the opposite limit of a fixed isotropic ensemble $q_1=q_2=0$.

According to Eqs. (5), (9), and (10) the a_{L_a} coefficient is $\propto q_2^2 f^2\mu_0^2$ and the dipolar terms in the expression of the b_{L_a} coefficient are $\propto q_1 f\mu_0$, where μ_0 is the real value of the dipole moment and f is the internal field factor (typically[15] $1.1<f<1.3$). In our Stark effect model, where $f=1$ was assumed, the a_{L_a} coefficient is $\propto\mu^2$ and the dipolar terms of the b_{L_a} coefficient are $\propto\mu^2$ and $\propto r\mu$. Thus, the parameters q_2 and q_1 are related to the fit parameters μ and r by

$$q_2=(\mu/f)/\mu_0, \tag{25}$$

$$q_1=r(\mu/f)/\mu_0=rq_2. \tag{26}$$

For indole and 3-MI in PMMA the restricted (unrelaxed) character of alignment manifests itself through about twice smaller internal-field-corrected value of the ground state dipole moment from the fit ($\mu/f=1.4/f$ D for indole and $1.3/f$ D for 3-MI) than its actual value [$\mu_0=2.1$ D for indole[27] and 3-MI (Ref. 33)]. As $r(\omega,T)=q_1/q_2$, the inequality $r<1$ indicates that in our experimental conditions ($\omega=40$ Hz and $T=20$ °C) the orientation component of the apparent field-induced angular distribution is suppressed in relation to the alignment component.

Although according to Eq. (11) the c_{L_a} coefficient and consequently the parameters $\Delta\mu_{L_a}$ and $\gamma=\boldsymbol{\Delta\mu}_{L_a}\angle\boldsymbol{\mu}$ are not sensitive to orientation/alignment, they can still be affected by the mathematics of the least-square fitting procedure. Therefore, for reliable determination of these parameters it is desirable to suppress the orientation/alignment effects, for example, by measuring at liquid nitrogen temperature.

B. Electric field effects on indole chromophore

In our Stark effect model the internal field factor f was assumed to be unity. It accounts for the enhancement in local field at the position of embedded molecule in relation to the applied electric field.[13,15,38] Based on theoretical estimates the f factor is believed to be of the order of 1.1–1.3.[11,13] Thus, the values of μ, $\Delta\mu_{L_a}$, $\Delta\alpha_{L_a}$, and $\Delta\alpha_{L_b}$ listed in Table II must be corrected by this factor if real values of these parameters are needed. For indole the corrected value of the dipole change, $\Delta\mu_{L_a}/f$, is in good agreement with the CASSCF/CASPT2 results on the ^1L_a state and the ground state dipole moments,[26,30] from which the dipole change can be estimated to range from 4 D to 5 D. The *ab initio* excited state dipole moments calculated at the ground state equilibrium geometry[26] seem to be more adequate for comparison with EA results. For the overview on earlier data on dipole change on the $^1L_a\leftarrow S_0$ transition of indole, determined mostly from the solvatochromic shifts, we refer to the work of Pierce and Boxer.[15]

Since the analysis of EA data yields only the value of $\cos\gamma=\cos(\boldsymbol{\Delta\mu}_{L_a}\angle\boldsymbol{\mu})$, there are still two alternatives for the direction of $\boldsymbol{\Delta\mu}_{L_a}$ with respect to the long axis of indole chromophore. The *ab initio* calculated directions of $\boldsymbol{\mu}_{L_a}$ and $\boldsymbol{\mu}$ for indole[26] suggest that $\boldsymbol{\Delta\mu}_{L_a}=\boldsymbol{\mu}_{L_a}-\boldsymbol{\mu}$ should be directed nearly along the long axis of indole chromophore as shown in Fig. 2. From $\gamma=34°$ (Table II) and from the known[27] angle of 40.5° between $\boldsymbol{\mu}$ and the long axis of in-

Downloaded 25 Aug 2004 to 129.100.61.167. Redistribution subject to AIP license or copyright, see http://jcp.aip.org/jcp/copyright.jsp

dole it follows that $\Delta\boldsymbol{\mu}_{L_a}$ is tilted from the long axis by 7° towards the nitrogen atom. Accepting that $\Delta\boldsymbol{\mu}_{L_a}$ lies nearly along the long axis and points from the benzene ring to the pyrrole ring for both indole and 3-MI, the electric field directed in the same way must cause redshift, but the field directed oppositely must cause blueshift of the ^1L_a absorption band as can be inferred from Eq. (3). Recent *ab initio* calculations of the term energies as a function of external electric field strength,[39] directed along the long, the short, and the perpendicular axis of indole confirm that the ^1L_a energy is most sensitive to the long axis component of the electric field.

Apart from the applied field the embedded molecules in a solvent or in a polymer host are exposed to the electric field caused by uneven distribution of charges in their local surrounding. Molecular dynamics simulations[2,10,39] of the water or the protein/water environment around the indole chromophore showed that the local electric field is strongly fluctuating and its mean strength is generally nonzero. Its instantaneous strength is of the order of tens of MV/cm.[2,39] This local field is responsible for the solvatochromic shift of the ^1L_a and ^1L_b absorption bands. In our case the ^1L_b band origin of indole (3-MI) was 4 nm (5 nm) redshifted from its gas-phase wavelength of 283.8 nm (Ref. 32) [286.7 nm (Ref. 40)]. In an EA experiment the applied Stark field is superimposed to the electric field produced by the local surrounding, i.e., a small change in absorption induced by the applied field is detected on the background of a much larger, but constant, spectral change (resulting from the average over the ensemble of absorbing molecules) induced by the local field.

Callis and Burgess[2] plotted the observed fluorescence maxima of tryptophan in different proteins as a function of the electric field the 3-MI part is subjected to, which was computed from the point charges and from the simulated by molecular dynamics geometry of a given protein/water surrounding (Fig. 1 in Ref. 2). A good correlation was achieved, characterized by the ratio of 1.3 MV/(cm·nm) between the strength of the long axis component of the electric field and the Stark shift $\Delta\lambda$. This result confirmed their internal Stark effect postulate, which states that the position of the fluorescence maximum for tryptophan in proteins is almost entirely determined by a single parameter: the projection of the average local electric field onto the dipole change in indole chromophore accompanying the $^1L_a \rightarrow S_0$ transition. The electric field strength relative to the Stark shift is directly related to $\Delta\mu_{L_a}$ via the equation $h\Delta\nu = \Delta\mu_{L_a} F$, which results in $\Delta\mu_{L_a} \approx 4.3$ D.

Ab initio caculations for indole[26,30,39,41] predicted the presence of Rydberg-type $^1A''(^1\pi\sigma^*)$ state, lying close to the ^1L_a and ^1L_b states. Owing to a large dipole moment[26,30] of 11 D its energetic location relative to the ^1L_a and ^1L_b states is very sensitive to an electric field, but owing to very low oscillator strength[26] of 3×10^{-5} the $^1\pi\sigma^* \leftarrow S_0$ absorption is negligible. Dedonder-Laredeux *et al.*[39] calculated the oscillator strengths for the transitions to the $^1\pi\sigma^*$, ^1L_a, and ^1L_b states as a function of the field strength for the field component perpendicular to the indole plane. For the field strength of 0.005 a.u. (26 MV/cm) the $^1L_a \leftarrow S_0$ oscillator strength was decreased from 0.07 to 0.06 owing to the field-induced mixing of the $^1\pi\sigma^*$, ^1L_a, and ^1L_b wave functions.[39] In the EA spectrum such a transition moment polarizability may appear as an extra zeroth-derivative ^1L_a contribution (of about -0.2 mO.D. for the field of 1 MV/cm). However, the decrease in the $^1L_a \leftarrow S_0$ oscillator strength should be accompanied by an increase in the $^1\pi\sigma^* \leftarrow S_0$ and $^1L_b \leftarrow S_0$ oscillator strengths, in a way that the sum oscillator strength is conserved. This implies that in an EA experiment the measured absorbance at a given wavelength is not changed in the presence of the electric field. It should be noted that the field-induced change in coupling with the $^1\pi\sigma^*$ state can appear in the *electrofluorescence* spectrum,[42,43] because the fluorescence intensity can be affected by the dissociation or by the internal conversion after the excitation.[39,41]

Lombardi[44,45] studied theoretically the field-induced ^1L_a and ^1L_b mixing in indole. In his Stark effect model a nondiagonal term of the Hamiltonian, $H_{12} = -\boldsymbol{\mu}_{L_aL_b}\cdot\mathbf{F}$, describing the energy of the transition dipole $\mu_{L_aL_b}$ between the ^1L_a and ^1L_b states in an electric field, was introduced besides the diagonal terms representing the energy of permanent dipoles. Applying his model to the solvatochromic data of indole[6] he obtained the following values of the dipoles: $\mu = 2.13$ D, $\mu_{L_b} = 2.39$ D, $\mu_{L_a} = 5.16$ D, and $\mu_{L_aL_b} = 0.27$ D. Unfortunately, our data are insufficient to confirm or disprove the nonzero value of $\mu_{L_aL_b}$.

The internal-field-corrected values of average polarizability change for indole and 3-MI, $\Delta\alpha_{L_a}/f^2$ and $\Delta\alpha_{L_b}/f^2$, are expected to be comparable with those for a molecule of similar size, for instance, naphthalene. For naphthalene the f-corrected values of the polarizability change on ^1L_a and ^1L_b excitation determined by the Stark spectroscopy are 9.8 Å^3 and 1.9 Å^3, respectively.[46] We admit that our $\Delta\alpha_{L_b}$ values can be overestimated, because they can include a contribution from the dipole change on $^1L_b \leftarrow S_0$ transition, $\Delta\mu_{L_b}$, which was neglected in our model. Finally we note that the average ground state polarizability of indole calculated at B3LYP/6-31+$G(d)$ level[47] is 98.7 a.u. (14.6 Å^3).

VI. SUMMARY

Room-temperature absorption and electroabsorption spectra are measured for indole and 3-MI, doped into a thin PMMA film. Measurements are performed at four different angles between the electric vector of the excitation light and the applied electric field, including the normal incidence case and the magic angle case.

An approximated subset of the Stark effect equations, accommodated to indole, is proposed. By fitting this model to the measured spectra of indole and 3-MI, the spectra are decomposed to the ^1L_a, ^1L_b, and ^1B_b constituents, and several parameters characterizing the indole chromophore subjected to the electric field in a PMMA environment are determined.

Changes in the EA spectrum depending on the angle between the light beam and the sample slide are reproduced by taking into account the alignment and orientation of the

Downloaded 25 Aug 2004 to 129.100.61.167. Redistribution subject to AIP license or copyright, see http://jcp.aip.org/jcp/copyright.jsp

polar indole (3-MI) molecules along the direction of the applied electric field. This proves that indole and 3-MI are *not immobilized* in a PMMA matrix at room temperature.

Field-induced dipolar *alignment* appeared in the normal incidence EA spectra as an absorbance decrease, whose spectrum is proportional to the ^1L_a absorption spectrum. Since for indole and 3-MI the ground state dipole moment and the ^1L_a transition dipole moment are almost parallel, the aligned ensemble of molecular dipoles absorbs the light, which is polarized perpendicularly to the applied field, less than the isotropic ensemble.

Field-induced dipolar *orientation* appeared in the EA spectra through the χ-dependent shift of the absorption band. In the magic angle case the apparent polarizability $\Delta\alpha_{L_a}^{\mathrm{eff}}$, which includes the dipolar orientation contribution, was six to seven times larger than the electronic polarizability change $\Delta\alpha_{L_a}$.

Smaller dipolar alignment contribution than expected on the basis of the known value of the ground state dipole moment, indicated that the angular mobility of indole and 3-MI is still restricted by the PMMA matrix. In other words, the orientational relaxation of indole (3-MI) in a PMMA matrix at room temperature is too slow for the angular distribution of the ground state molecular dipoles to follow in a full extent the instantaneous strength of 40 Hz ac Stark field.

The obtained values of $\Delta\mu_{L_a}$ (the change in dipole moment on the ^1L_a transition *not corrected* by the internal field factor) are 5.6 D for indole and 7.2 D for 3-MI.

Our results confirm that for indole and 3-MI the dipole change $\boldsymbol{\Delta\mu}_{L_a}$ is directed from the benzene ring to the pyrrole ring nearly along the long axis of indole chromophore. For indole the tilt angle of $\boldsymbol{\Delta\mu}_{L_a}$ from the long axis towards the nitrogen atom is confined in the range from 0° to 14°.

Two possible directions for future research emerge from this study: EA study of the electronic properties of indoles immobilized in a frozen host matrix and EA study of the field-induced orientation/alignment effects in a polymer film at various sample conditions (using a polar test molecule with a less complicated electronic structure).

ACKNOWLEDGMENTS

E.J. is thankful to A. L. Sobolewski and S. Perun for their *ab initio* results and to the Japan Society for the Promotion of Science (JSPS) for funding his research stay in Hokkaido Univerity. This work was supported by the Grants-in-Aid for Scientific Research (A) (2) (15205001) and for Scientific Research on Priority Area (417) from the Ministry of Education, Culture, Sports, Science and Technology of Japan and partially by the Estonian Science Foundation (Grant No. 5044).

[1] J. T. Vivian and P. R. Callis, Biophys. J. **80**, 2093 (2001).
[2] P. R. Callis and B. K. Burgess, J. Phys. Chem. B **101**, 9429 (1997).
[3] P. R. Callis, Methods Enzymol. **278**, 113 (1997).
[4] K. W. Short and P. R. Callis, J. Chem. Phys. **113**, 5235 (2000).
[5] E. H. Strickland, J. Horwitz, and C. Billups, Biochemistry **9**, 4914 (1970).
[6] H. Lami and N. Glasser, J. Chem. Phys. **84**, 597 (1986).
[7] J. Catalán and C. Díaz, Chem. Phys. Lett. **368**, 717 (2003).
[8] S. R. Meech, D. Phillips, and A. G. Lee, Chem. Phys. **80**, 317 (1983).
[9] N. Mataga, Y. Torihashi, and K. Ezumi, Theor. Chim. Acta **2**, 158 (1964).
[10] P. L. Muiño and P. R. Callis, J. Chem. Phys. **100**, 4093 (1994).
[11] G. U. Bublitz and S. G. Boxer, Annu. Rev. Phys. Chem. **48**, 213 (1997).
[12] W. Liptay, in *Excited States*, edited by E. C. Lim (Academic, New York, 1974), Vol. 1, p. 129.
[13] M. Ponder and R. Mathies, J. Phys. Chem. **87**, 5090 (1983).
[14] S. A. Locknar and L. A. Peteanu, J. Phys. Chem. B **102**, 4240 (1998).
[15] D. W. Pierce and S. G. Boxer, Biophys. J. **68**, 1583 (1995).
[16] B. Valeur and G. Weber, Photochem. Photobiol. **25**, 441 (1977).
[17] M. R. Eftink, L. A. Selvidge, P. R. Callis, and A. A. Rehms, J. Phys. Chem. **94**, 3469 (1990).
[18] R. L. Rich, Y. Chen, D. Neven, M. Négrerie, F. Gai, and J. W. Petrich, J. Phys. Chem. **97**, 1781 (1993).
[19] N. Ohta, S. Okazaki, and I. Yamazaki, Chem. Phys. Lett. **229**, 394 (1994).
[20] N. Ohta, T. Ito, S. Okazaki, and I. Yamazaki, J. Phys. Chem. B **101**, 10213 (1997).
[21] N. Ohta, Y. Iwaki, T. Ito, I. Yamazaki, and A. Osuka, J. Phys. Chem. B **103**, 11242 (1999).
[22] T. A. Osswald and G. Menges, *Materials Science of Polymers for Engineers* (Hanser, Munich, 1995).
[23] G. U. Bublitz, R. Ortiz, S. R. Marder, and S. G. Boxer, J. Am. Chem. Soc. **119**, 3365 (1997).
[24] F. W. Vance, R. D. Williams, and J. T. Hupp, Int. Rev. Phys. Chem. **17**, 307 (1998).
[25] C.-T. Chang, C.-Y. Wu, A. R. Muirhead, and J. R. Lombardi, Photochem. Photobiol. **19**, 347 (1974).
[26] A. L. Sobolewski and W. Domcke, Chem. Phys. Lett. **315**, 293 (1999).
[27] W. Caminati and S. Di Bernardo, J. Mol. Struct. **240**, 253 (1990).
[28] L. S. Slater and P. R. Callis, J. Phys. Chem. **99**, 8572 (1995).
[29] B. Albinsson and B. Nordén, J. Phys. Chem. **96**, 6204 (1992).
[30] L. Serrano-Andrés and B. O. Roos, J. Am. Chem. Soc. **118**, 185 (1996).
[31] A. C. Borin and L. Serrano-Andrés, Chem. Phys. **262**, 253 (2000).
[32] G. Berden, E. Jalviste, and W. L. Meerts, J. Chem. Phys. **103**, 9596 (1995).
[33] J. Carney, F. C. Hagemeister, and T. S. Zwier, J. Chem. Phys. **108**, 3379 (1998).
[34] A. Chowdhury, S. A. Locknar, L. L. Premvardhan, and L. A. Peteanu, J. Phys. Chem. A **103**, 9614 (1999).
[35] A. Z. Britten and G. L. Lockwood, Spectrochim. Acta, Part A **32**, 1335 (1976).
[36] S. Saal and W. Haase, Chem. Phys. Lett. **278**, 127 (1997).
[37] S. A. Locknar, A. Chowdhury, and L. A. Peteanu, J. Phys. Chem. B **104**, 5816 (2000).
[38] L. Premvardhan and L. Peteanu, Chem. Phys. Lett. **296**, 521 (1998).
[39] C. Dedonder-Lardeux, C. Jouvet, S. Perun, and A. L. Sobolewski, Phys. Chem. Chem. Phys. **5**, 5118 (2003). In the axis convention given by Fig. 2 in this reference the direction of *Y* axis must be reversed.
[40] K. Remmers, E. Jalviste, I. Mistrík, G. Berden, and W. L. Meerts, J. Chem. Phys. **108**, 8436 (1998).
[41] A. L. Sobolewski, W. Domcke, C. Dedonder-Lardeux, and C. Jouvet, Phys. Chem. Chem. Phys. **4**, 1093 (2002).
[42] N. Ohta, Bull. Chem. Soc. Jpn. **75**, 1637 (2002).
[43] N. Ohta, M. Koizumi, S. Umeuchi, Y. Nishimura, and I. Yamazaki, J. Phys. Chem. **100**, 16466 (1996).
[44] J. R. Lombardi, J. Phys. Chem. A **102**, 2817 (1998).
[45] J. R. Lombardi, J. Phys. Chem. A **103**, 6335 (1999).
[46] R. Mathies and A. C. Albrecht, J. Chem. Phys. **60**, 2500 (1974).
[47] K. R. F. Somers, E. S. Kryachko, and A. Ceulemans, Chem. Phys. **301**, 61 (2004).

Downloaded 25 Aug 2004 to 129.100.61.167. Redistribution subject to AIP license or copyright, see http://jcp.aip.org/jcp/copyright.jsp